Kinetochore-mediated outward force promotes spindle pole separation in fission yeast

Yutaka Shirasugi[a] and Masamitsu Sato[a,b,c,*]
[a]Laboratory of Cytoskeletal Logistics, Department of Life Science and Medical Bioscience, [b]Institute for Medical-Oriented Structural Biology, and [c]Institute for Advanced Research of Biosystem Dynamics, Waseda Research Institute for Science and Engineering, School of Advanced Science and Engineering, Waseda University, TWIns, 2-2 Wakamatsucho, Shinjuku-ku, Tokyo 162-8480, Japan

ABSTRACT **Bipolar spindles are organized by motor proteins that generate microtubule-dependent forces to separate the two spindle poles. The fission yeast Cut7 (kinesin-5) is a plus-end-directed motor that generates the outward force to separate the two spindle poles, whereas the minus-end-directed motor Pkl1 (kinesin-14) generates the inward force. Balanced forces by these antagonizing kinesins are essential for bipolar spindle organization in mitosis. Here, we demonstrate that chromosomes generate another outward force that contributes to the bipolar spindle assembly. First, it was noted that the *cut7 pkl1* double knockout failed to separate spindle poles in meiosis I, although the mutant is known to succeed it in mitosis. It was assumed that this might be because meiotic kinetochores of bivalent chromosomes joined by cross-overs generate weaker tensions in meiosis I than the strong tensions in mitosis generated by tightly tethered sister kinetochores. In line with this idea, when meiotic mono-oriented kinetochores were artificially converted to a mitotic bioriented layout, the *cut7 pkl1* mutant successfully separated spindle poles in meiosis I. Therefore, we propose that spindle pole separation is promoted by outward forces transmitted from kinetochores to spindle poles through microtubules.**

Monitoring Editor
Kerry S. Bloom
University of North Carolina

Received: Jul 12, 2019
Revised: Sep 6, 2019
Accepted: Sep 10, 2019

INTRODUCTION

Chromosome segregation is driven by a bipolar spindle, which consists of microtubules emanating from spindle poles. Bipolar spindle assembly is regulated by outward pushing forces and inward pulling forces generated by microtubules and microtubule-associated proteins (MAPs). The plus-end-directed motor kinesin-5 (BimC/Eg5/Cut7) cross-links and slides antiparallel microtubules, thereby pushing away the two spindle poles harboring minus ends of the microtubules (Kashina *et al.*, 1996; Kapitein *et al.*, 2005).

The outward force generated by kinesin-5 is essential for bipolar spindle assembly, as its inhibition results in monopolar spindles, defined by a failure in separation of the two spindle poles (Hagan and Yanagida, 1990, 1992; Heck *et al.*, 1993; Mayer *et al.*, 1999; Kapoor *et al.*, 2000). On the contrary, inward forces are generated by minus-end-directed motors such as kinesin-14 and dynein (Sharp *et al.*, 1999; Mitchison *et al.*, 2005). Outward and inward forces are antagonistic to each other during spindle pole separation. The monopolar spindle caused by kinesin-5 inhibition is canceled by the simultaneous depletion of kinesin-14 or dynein in humans, *Drosophila*, *Xenopus* eggs, and fission yeast (Pidoux *et al.*, 1996; Sharp *et al.*, 1999; Troxell *et al.*, 2001; Mitchison *et al.*, 2005; Tanenbaum *et al.*, 2008; Ferenz *et al.*, 2009; Olmsted *et al.*, 2014; van Heesbeen *et al.*, 2014). The interplay of the kinesin-5 and kinesin-14 in bipolar spindle assembly was intensively investigated in the fission yeast *Schizosaccharomyces pombe*.

Fission yeast has a kinesin-5 protein Cut7 and two kinesin-14 proteins; Pkl1 and Klp2 (Hagan and Yanagida, 1990; Pidoux *et al.*, 1996; Troxell *et al.*, 2001). Cut7 generates an outward force that slides antiparallel microtubules apart (Hagan and Yanagida, 1990, 1992) (see Figure 1A for a schematic, left). Cut7 is essential for the separation of spindle pole bodies (SPBs, the fungal equivalent of

This article was published online ahead of print in MBoC in Press (http://www.molbiolcell.org/cgi/doi/10.1091/mbc.E19-07-0366) on September 18, 2019.

*Address correspondence to: Masamitsu Sato (masasato@waseda.jp).

Abbreviations used: cnt, central core region; DAPI, 4′,6-diamidino-2-phenylindole; GFP/YFP/CFP, green/yellow/cyan fluorescent protein; MAP, microtubule-associated protein; SPA, sporulation agar; SPB, spindle pole body; WT, wild type.

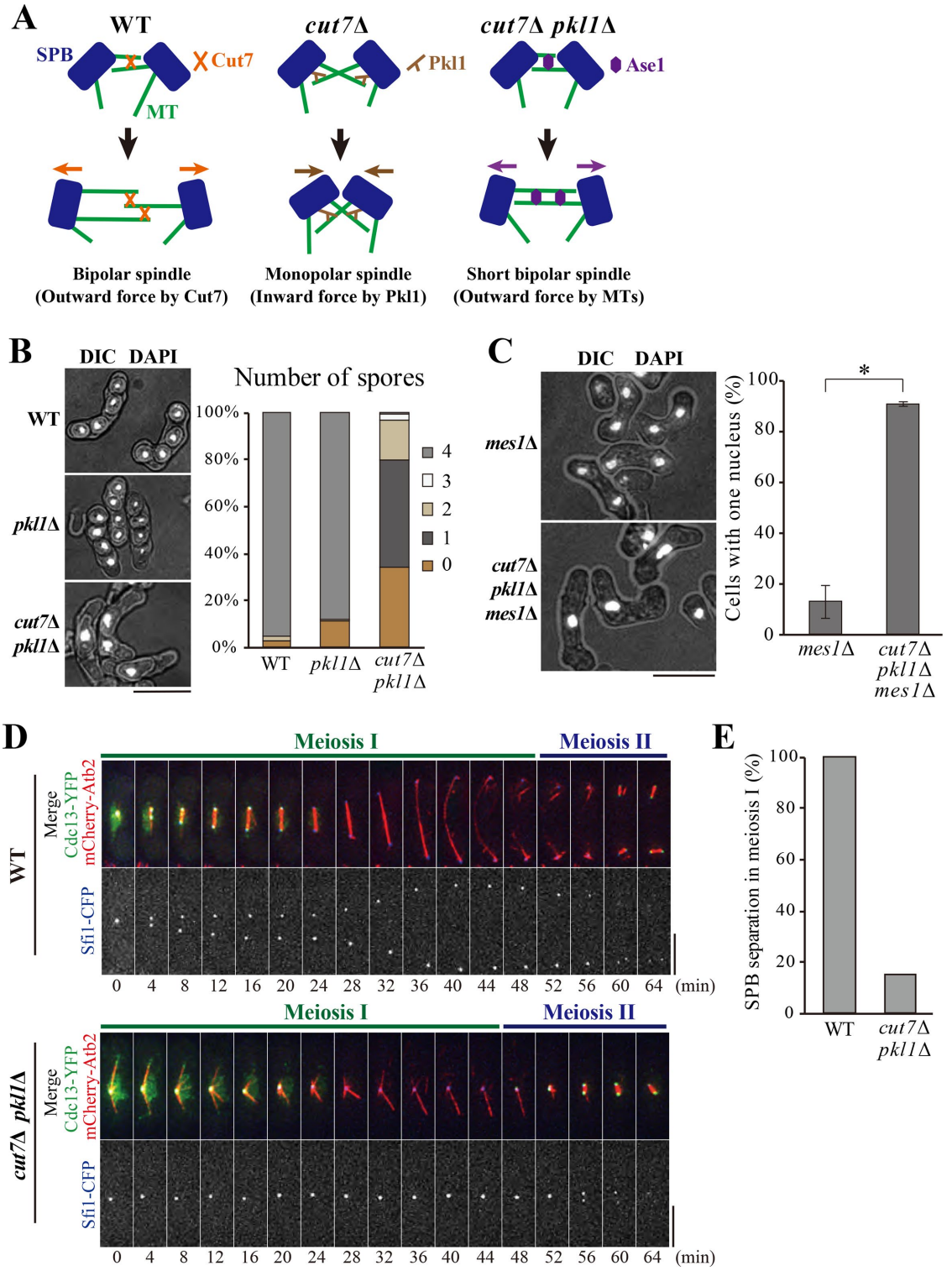

FIGURE 1: *cut7Δ pkl1Δ* cells display the monopolar spindle in meiosis I. (A) Schematics for spindle assembly in the mitosis of WT, *cut7Δ*, and *cut7Δ pkl1Δ* cells. (B) The *cut7Δ pkl1Δ* cells are defective in meiosis and sporulation. Cells of indicated genotypes were stained with DAPI. Images are shown merged with differential interference contrast (DIC) (left). The spores in an ascus were counted (right, WT, $n = 111$ cells; *pkl1Δ*, $n = 108$ cells; *cut7Δ pkl1Δ*, $n = 131$ cells). Scale bar, 10 μm. (C) Meiosis was induced for *mes1Δ* and *cut7Δ pkl1Δ mes1Δ* cells. Cells were stained with DAPI, and the chromosome masses in a zygote were counted (mean ± SD $n > 94$ cells, $N = 2$ experiments). Scale bar, 10 μm. *$P < 0.005$ (Welch's *t* test). (D) Living cells expressing Cdc13-YFP (green), mCherry-Atb2 (microtubules; red), and Sfi1-CFP (SPB; blue) were observed from the onset of meiosis I in WT (top) and *cut7Δ pkl1Δ* (bottom). The value 0 min corresponds to the start of time-lapse imaging. Scale bars, 5 μm. (E) Percentages of WT and *cut7Δ pkl1Δ* cells that showed SPB separation in meiosis I were calculated from observation in C (WT, $n = 11$ cells; *cut7Δ pkl1Δ*, $n = 13$ cells).

the centrosome) (Hagan and Yanagida, 1990, 1992), and the deletion mutant of Cut7 (*cut7*Δ) is lethal. The conditional (temperature-sensitive) mutant of Cut7 shows the monopolar spindle phenotype at the restrictive temperature, which is a hallmark of SPB separation defects. In contrast, Pkl1 localizes closely to SPBs and generates an inward force that pulls microtubules emanating from opposite poles (Rincon *et al*., 2017; Yukawa *et al*., 2017, 2018) (Figure 1A, center).

The lethality of *cut7*Δ is suppressed by the deletion of the *pkl1* gene; and the *cut7*Δ *pkl1*Δ double mutant survives (Olmsted *et al*., 2014) and manages to eventually separate SPBs by microtubules grown in a later stage than usually seen in wild type (WT) cells (Rincon *et al*., 2017; Yukawa *et al*., 2017). The *cut7*Δ *pkl1*Δ double mutant utilizes the antiparallel microtubule bundling factor Ase1/PRC1 for SPB separation (Rincon *et al*., 2017; Yukawa *et al*., 2017). Ase1 in WT cells generates outward pushing forces in the spindle midzone in anaphase that contributes to elongation of the anaphase spindle (Loïodice *et al*., 2005; Yamashita *et al*., 2005) (Figure 1A, right). In silico simulations suggest that the Ase1-dependent mechanism is seemingly sufficient for bipolar spindle assembly in the absence of Cut7 and Pkl1 (Rincon *et al*., 2017). Therefore, the force balance exerted for the positioning of two SPBs can be explained by Cut7, Pkl1, and additional factors located on interpolar microtubules connecting two SPBs.

In addition to recent knowledge, we here propose an additional outward force that may contribute to the separation of SPBs in the pro-prometaphase of mitosis. Chromosomes play a key role in outward force generation. In mitosis, kinetochores located on sister chromatids are bioriented to associate with microtubules from opposite poles. In the first division of meiosis (meiosis I), homologous chromosomes are paired as bivalent with some cross-overs as a result of meiotic recombination (reviewed in Siomos and Nasmyth, 2003; Yamagishi *et al*., 2014). Spindle microtubules need to segregate homologues but not sister chromatids. For this purpose, sister kinetochores are tightly tethered throughout meiosis I by the meiotic cohesin Rec8 as well as the monopolin Moa1, so that such mono-oriented sister kinetochores can be associated to microtubules from either of the two SPBs (Yokobayashi and Watanabe, 2005). When spindle microtubules attach to kinetochores to pull them, bivalent chromosomes are stretched by pulling forces generated in the spindle (reviewed in Nicklas, 1974).

In this study, we use mitotic and meiotic cells to investigate how chromosomes affect SPB separation. Through analyses, we propose that kinetochores attached to microtubules provide mechanical support to push SPBs apart during the pro-prometaphase of mitosis.

RESULTS

*cut7*Δ *pkl1*Δ cells fail to assemble the bipolar spindle in meiosis I

Recent knowledge regarding the force balance is summarized as a schematic in Figure 1A. Cut7 is essential for SPB separation in fission yeast (Hagan and Yanagida, 1990, 1992). The *cut7* deletion mutant (*cut7*Δ) is inviable as it is unable to separate SPBs, but the *cut7*Δ *pkl1*Δ double mutant is shown to be viable (Olmsted *et al*., 2014) (Supplemental Figure S1A). Indeed, *cut7*Δ *pkl1*Δ cells separate SPBs, albeit partially, powered by the sliding of interdigitating microtubules with the assistance of the microtubule cross-linker Ase1 (Rincon *et al*., 2017; Yukawa *et al*., 2017) (Figure 1A and Supplemental Figure S1, B and C). The spindles in *cut7*Δ *pkl1*Δ cells were elongated later in the anaphase, although the timing appeared delayed compared with those in WT cells (Rincon *et al*., 2017; Yukawa *et al*., 2017) (Supplemental Figure S1, B and C).

However, it was found that the *cut7*Δ *pkl1*Δ mutant showed severe defects in meiotic progression. Although WT and *pkl1*Δ zygotes underwent normal meiosis and produced four spores, *cut7*Δ *pkl1*Δ zygotes mostly produced 0–2 spores per ascus (Figure 1B). The number of nuclei indicated by DAPI (4′,6-diamidino-2-phenylindole) was one or two in most asci, instead of four in WT asci as a result of two rounds of meiotic divisions (meiosis I and II). This result indicates that the *cut7*Δ *pkl1*Δ mutant is deficient in chromosome segregation in meiosis.

The *mes1*Δ mutation, which arrests meiotic progression before meiosis II at the binucleate state, was utilized for further clarification studies (Bresch *et al*., 1968; Izawa *et al*., 2005) (Figure 1C). In contrast, ~90% of *cut7*Δ *pkl1*Δ *mes1*Δ zygotes showed one nucleus (Figure 1C), indicating that cells were unable to undergo meiosis I in the simultaneous absence of Cut7 and Pkl1.

Therefore, the progression of meiosis I by the time-lapse imaging of WT and *cut7*Δ *pkl1*Δ cells expressing Cdc13-YFP (cyclin B) (Decottignies *et al*., 2001), mCherry-Atb2 (α2-tubulin) (Sato *et al*., 2009), and Sfi1-CFP (a component of the SPB half-bridge) (Kilmartin, 2003) was investigated. In WT cells, SPBs separated and accordingly, the bipolar spindle was formed by the metaphase of meiosis I (4 min onward; note that Cdc13-YFP localized to SPBs; Figure 1D, top). Cdc13 then disappeared, and the spindle began to elongate on entry into the anaphase (24 min). In contrast, SPBs failed to separate in 85% of the *cut7*Δ *pkl1*Δ cells, and the resulting monopolar spindle remained until the end of meiosis I when Cdc13-YFP disappeared (Figure 1, D and E, bottom).

Despite the failure in bipolar spindle formation in meiosis I, it appeared that the SPBs separated and the bipolar spindle was assembled later, in the timing of meiosis II (56 min, Figure 1D, bottom), which was indicated by the reaccumulation of Cdc13-YFP on SPBs. Although the spindle for meiosis II started to assemble, it failed to fully elongate and segregate chromosomes. Therefore, most of the mutant cells produced a single spore with a single nucleus (Figure 1, B and D). Taking these results together, it was concluded that the Cut7-independent spindle assembly machinery that operates in mitosis might not properly function in meiosis I.

Deletion of *klp2* improves the SPB separation of *cut7*Δ *pkl1*Δ cells in meiosis I

It was then hypothesized that the monopolar spindle phenotype seen in meiosis I of the *cut7*Δ *pkl1*Δ mutant was due to the imbalance of spindle forces. The inward forces pulling SPBs might be strong relative to outward pushing forces in the meiosis I spindle. To test this hypothesis, the deletion of the *klp2* gene was introduced. While the kinesin-5 Cut7 generates an outward force, two kinesin-14 proteins, Pkl1 and Klp2, generate inward forces in the mitotic spindle (Rincon *et al*., 2017; Yukawa *et al*., 2017, 2018, 2019). In line with this, previous observations for mitosis have demonstrated that the bipolar spindle assembled in *cut7*Δ *pkl1*Δ cells is ameliorated even by the simultaneous deletion of *klp2* (Yukawa *et al*., 2018, 2019).

Therefore, meiosis I of the *cut7*Δ *pkl1*Δ *klp2*Δ triple knockout cells was observed. First, most of the *cut7*Δ *pkl1*Δ cells failed to undergo meiosis I resulting in improper nuclear division, as shown above (Figures 1 and 2A). In contrast, ~40% of the *cut7*Δ *pkl1*Δ *klp2*Δ cells generated four spores with four nuclei as WT cells did (Figure 2A), indicating that defects in SPB separation were canceled by the additional deletion of *klp2*. As expected, similar percentages of *cut7*Δ *pkl1*Δ *klp2*Δ cells separated SPBs and assembled the bipolar spindle by metaphase of meiosis I (12 min; Figure 2, B and C, bottom), followed by spindle elongation in the anaphase (40 min).

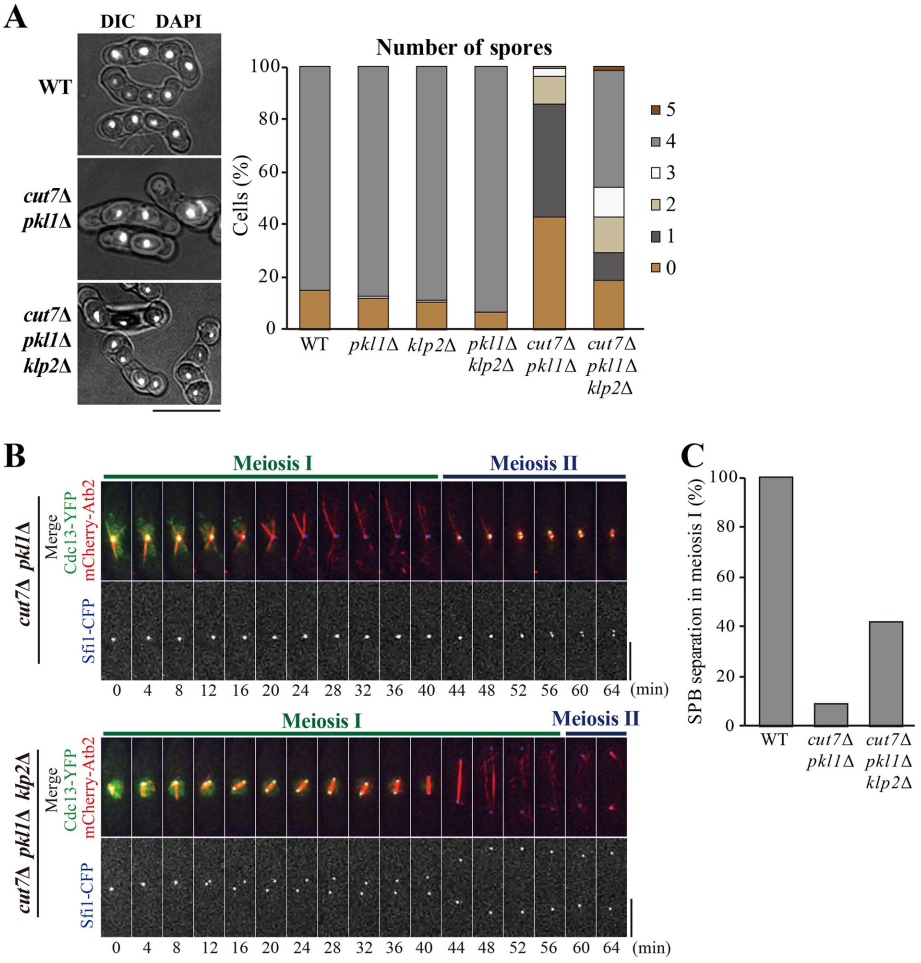

FIGURE 2: Deletion of *klp2* partly suppresses meiotic defects in *cut7*Δ *pkl1*Δ. (A) Sporulation was monitored in the cells of indicated genotypes. Cells were stained with DAPI and shown with DIC (left). Proportions of the number of spores are also shown (right, WT, $n = 183$ cells; *pkl1*Δ, $n = 181$; *klp2*Δ, $n = 89$; *pkl1*Δ *klp2*Δ, $n = 146$; *cut7*Δ *pkl1*Δ, $n = 179$; *cut7*Δ *pkl1*Δ *klp2*Δ, $n = 151$). Scale bar, 10 μm. (B) Cells expressing Cdc13-YFP (green), mCherry-Atb2 (microtubules; red), and Sfi1-CFP (SPB; blue) were observed from the onset of meiosis I in *cut7*Δ *pkl1*Δ (top) and *cut7*Δ *pkl1*Δ *klp2*Δ (bottom). Scale bars, 5 μm. (C) Percentages of WT, *cut7*Δ *pkl1*Δ, and *cut7*Δ *pkl1*Δ *klp2*Δ cells that showed SPB separation in meiosis I were calculated from observations in B (WT, $n = 12$ cells; *cut7*Δ *pkl1*Δ, $n = 11$; *cut7*Δ *pkl1*Δ *klp2*Δ, $n = 12$).

These results demonstrate that *cut7*Δ *pkl1*Δ cells were unable to separate SPBs in meiosis I because of the imbalance of forces inside the spindle that was not evident during mitotic divisions.

Chromosome configuration affects the balance of forces inside the meiotic spindle

Collectively, these results indicate that in meiosis I, the inward forces are stronger or outward forces are weaker than in mitosis. Therefore, *cut7*Δ *pkl1*Δ cells fail to separate SPBs in meiosis I.

As a result, the reasons why the force imbalance was evident, particularly in meiosis I, were examined. This difference could be due to the ploidy of cells used in the experiments, as current knowledge on mitosis has been based on observations using haploid cells, and the meiotic cells used in this study are diploid. The diploid *cut7*Δ *pkl1*Δ strain was constructed for the observation of mitosis to test this possibility. Diploid cells of *cut7*Δ *pkl1*Δ showed SPB separation and bipolar spindle formation in mitosis (Supplemental Figure S2, A and B), as seen in haploid cells (Olmsted *et al.*, 2014). Hence, ploidy cannot be the reason for the monopolar spindle phenotype seen in meiosis I of the *cut7*Δ *pkl1*Δ cells.

Next, it was considered that chromosome configuration in meiosis I may cause the force imbalance. In mitosis and meiosis II, sister chromatids are tied together with cohesin, whereas homologous chromosomes behave independently. On the contrary, homologues are paired, and cross-overs are made prior to meiosis I (reviewed in Moore, 1998; Siomos and Nasmyth, 2003). The bivalent chromosomes with chiasmata are associated with microtubules so that homologues are separated in meiosis I (WT; see Figure 3A for a schematic). In each type of division, chromosome configuration is correlated with the SPB state in *cut7*Δ *pkl1*Δ cells. Namely, SPBs separated in mitosis and meiosis II, but not in meiosis I (see Figure 1D).

This indicated that chromosomes associated with the spindle might act as a pivot point for the spindle structure. The fulcrum of the pivot point could be kinetochores, as they form the site for physical attachment to microtubules.

The polarity of kinetochores is key for outward force generation

In mitosis and meiosis II, kinetochores of sister chromatids are oriented in a back-to-back configuration (Mitosis, Figure 3A) called biorientation (reviewed in Yamagishi *et al.*, 2014). In meiosis I, sister kinetochores are united so that microtubules from either of the spindle poles can associate (mono-orientation), and homologues are paired as bivalent in a tetrad connected by cross-overs (Meiosis I, WT, Figure 3A).

SPO11/Rec12 is a protein that introduces double-strand breaks to meiotic chromosomes, thereby facilitating meiotic cross-overs and pairing (Cao *et al.*, 1990; Lin and Smith, 1994; Keeney *et al.*, 1997; Cervantes *et al.*, 2000). In the absence of SPO11/Rec12, homologues are never paired (called univalent), although kinetochores remain mono-oriented (*rec12*Δ, Figure 3A) (Yokobayashi and Watanabe, 2005; Sakuno *et al.*, 2011). The monopolin protein Moa1 is responsible for the mono-orientation of sister kinetochores in meiosis I (Yokobayashi and Watanabe, 2005). Therefore, the removal of Moa1 in *rec12*Δ cells causes the biorientation of sister kinetochores without forming a bivalent to mimic the chromosome configuration of mitosis (*rec12*Δ *moa1*Δ, Figure 3A).

To investigate whether chromosome configuration in meiosis I causes the force imbalance in *cut7*Δ *pkl1*Δ cells, Rec12 was first removed from the cells and disconnected homologues. The majority of *cut7*Δ *pkl1*Δ *rec12*Δ cells (~90%) terminated meiosis I without separating SPBs, as in *cut7*Δ *pkl1*Δ cells, suggesting that chiasma formation per se is not the reason for force imbalance (*cut7*Δ *pkl1*Δ *rec12*Δ, Figure 3, B and C). When Rec12 and Moa1 were simultaneously removed from *cut7*Δ *pkl1*Δ cells, 52% of the cells successfully separated SPBs in meiosis I (16 min,

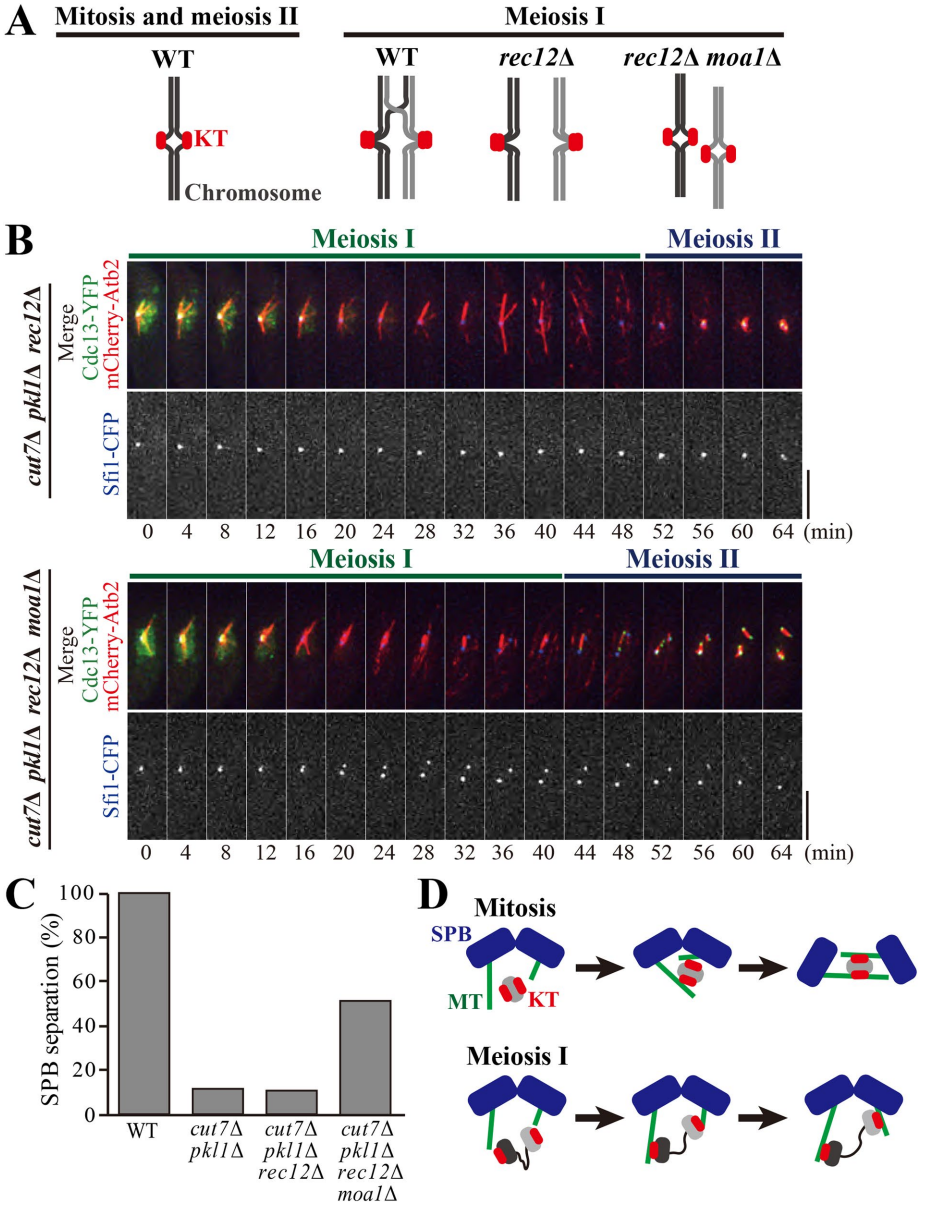

FIGURE 3: Deletion of Rec12 and Moa1 suppresses defects in the SPB separation of *cut7Δ pkl1Δ* cells. (A) Schematics for chromosome configuration in mitosis (WT) and meiosis I of WT, *rec12Δ*, and *rec12Δ moa1Δ* cells. For meiosis I, a pair of homologous chromosomes (black and gray) are shown. Red, kinetochores (KT) (B) Cells expressing Cdc13-YFP (green), mCherry-Atb2 (microtubules; red), and Sfi1-CFP (SPB; blue) were observed from the onset of meiosis I in *cut7Δ pkl1Δ rec12Δ* (top) and *cut7Δ pkl1Δ rec12Δ moa1Δ* (bottom). Scale bars, 5 μm. (C) Percentages of cells that showed the separation of SPBs in meiosis I in indicated strains, as calculated from observations in B (WT, $n = 10$ cells; *cut7Δ pkl1Δ*, $n = 17$; *cut7Δ pkl1Δ rec12Δ*, $n = 9$; *cut7Δ pkl1Δ rec12Δ moa1Δ*, $n = 25$). (D) Models as to how kinetochores serve as a fulcrum for microtubules emanated from two SPBs. Mitosis, gray ovals indicate sister chromatids of a chromosome. Meiosis I, Gray and black ovals denote homologous chromosomes in a bivalent, the kinetochores of which are loosely connected (denoted by a wavy line). Green filaments denote microtubules (MT).

cut7Δ pkl1Δ rec12Δ moa1Δ; Figure 3, B and C). Therefore, the conversion of chromosome configuration from meiosis I to mitosis rebalanced the forces inside the spindle.

In *moa1Δ* cells, sister kinetochores are converted to the bioriented pattern in meiosis I, although homologous chromosomes are still tied as bivalent (Yokobayashi and Watanabe, 2005) (Supplemental Figure S3A). The *cut7Δ pkl1Δ moa1Δ* cells frequently recovered SPB separation in meiosis I, which is similar to the case of *cut7Δ pkl1Δ rec12Δ moa1Δ* cells (Supplemental Figure S3, B and C). This means that the biorientation of kinetochores, no matter whether bivalent or univalent, drives the outward force for SPB separation.

Therefore, artificially bioriented kinetochores restore SPB separation in meiosis I lack both Cut7 and Pkl1. Although *cut7Δ pkl1Δ* cells without Klp2 and Rec12–Moa1 both showed SPB separation in the prometaphase of meiosis I, they showed distinct behavior in spindle elongation later in the anaphase. The *cut7Δ pkl1Δ klp2Δ* successfully elongated the spindle (see Figure 2B), whereas *cut7Δ pkl1Δ rec12Δ moa1Δ* (and *cut7Δ pkl1Δ moa1Δ*) failed to do so, which instead resulted in spindle collapse (28–32 min, Figure 3B, and 24–28 min, Supplemental Figure S3B). As both *moa1Δ* and *rec12Δ moa1Δ* cells often displayed lagging chromosomes in the anaphase because of merotelic attachment between microtubules and kinetochores (Yokobayashi and Watanabe, 2005), anaphase spindle elongation might be hampered in those mutants including *moa1Δ*.

In conclusion, in meiosis I without Cut7 and Pkl1, the outward forces that separate SPBs are not fully generated because of the mono-oriented kinetochores of bivalent chromosomes.

In mitosis, sister kinetochores attach to microtubules emanating from two SPBs. Then, kinetochores might be able to serve as a fulcrum for microtubules to generate a repulsive force for SPB separation (Mitosis, Figure 3D). Notably, the bipolar attachment of microtubules to kinetochores is not fully established in the early stages of mitosis. Therefore, the kinetochore-mediated outward force may not be generated through the "end-on" attachment of microtubules to kinetochores. Instead, sister kinetochores first attach to the lateral surfaces of microtubules from two SPBs. Even before conversion to end-on attachment, lateral attachment might be able to interlock the antiparallel microtubules, thereby generating the repulsive force for SPB separation (Figure 3D; see *Discussion*).

In this context, the force imbalance in *cut7Δ pkl1Δ* cells during meiosis I may be interpreted as a lack of the repulsive force at kinetochores because homologous kinetochores in a bivalent are relaxed. Figure 3D (Meiosis I) illustrates this situation; gray and black ovals denote homologous chromosomes of a bivalent, and their kinetochores are loosely connected (drawn as a wavy line).

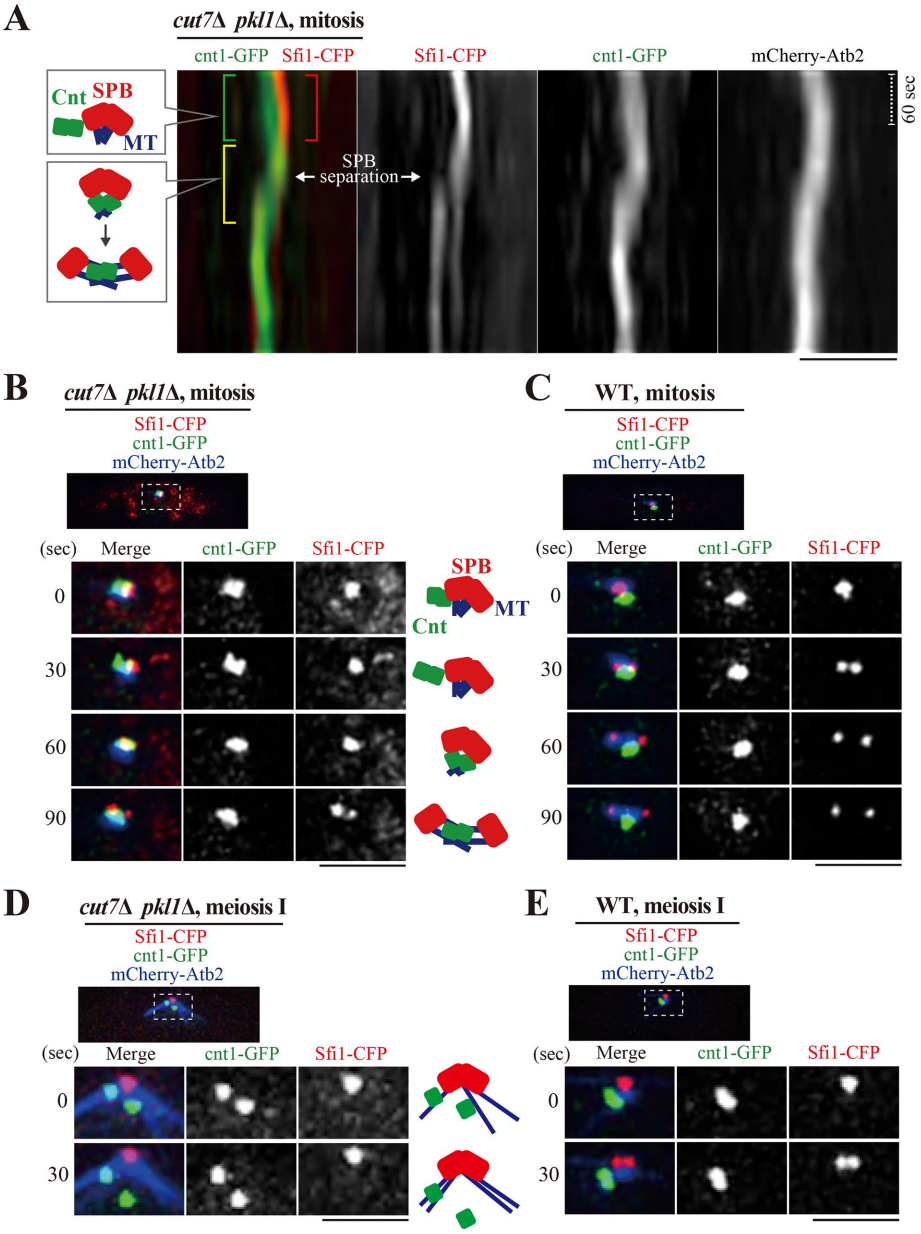

FIGURE 4: Position of kinetochores and SPBs in mitosis and meiosis I. Location of SPBs (Sfi1-CFP; red) and centromeres of chromosome 1 (cnt1-GFP; green) together with microtubules (mCherry-Atb2; blue) were visualized in the *cut7Δ pkl1Δ* and WT cells. (A, B) A representative *cut7Δ pkl1Δ* cell in mitosis. The positional relationship between kinetochores and SPBs over time is shown in kymographs (A) and in time-lapse sequential images (B). In kymographs (A), the mCherry-Atb2 image is not merged. Green and red brackets denote separate positioning of cnt1-GFP and Sfi1-CFP. A yellow bracket denotes overlap of cnt1-GFP and Sfi1-CFP signals. The timing of SPB separation is pinpointed. Corresponding schematics for SPBs, centromeres (Cnt), and microtubules are illustrated (left). The dotted line corresponds to 60 s. In B, the dotted inset is shown below as time-lapse images. Corresponding schematics are shown (right). Time 0 is defined as when nuclear microtubules started to assemble. (C) A mitotic WT cell. (D, E) *cut7Δ pkl1Δ* (D) and WT (E) cells on entry into meiosis I. Scale bars, 2 μm.

Kinetochore positioning affects the generation of a repulsive force for SPB separation

The cnt1-GFP system was employed to investigate whether kinetochores indeed generate the repulsive force to separate SPBs. The central core regions (cnt) of the centromeres in chromosome 1 were selectively visualized with GFP (Sakuno *et al.*, 2009). We monitored the positional relationship between sister kinetochores (cnt1-GFP) and SPBs (Sfi1-CFP) when *cut7Δ pkl1Δ* (and WT) cells enter mitosis (Figure 4, A–C). Figure 4A displays kymographs derived from images of the *cut7Δ pkl1Δ* cells shown in Figure 4B. Although cnt1-GFP (green) and SPBs (red) were closely located, on entry into mitosis, the cnt1-GFP foci stood aside two SPBs (0–30 s, Figure 4B). In the corresponding kymographs (Figure 4A), the green and red brackets denote separate side-by-side positioning of sister kinetochores and SPBs, which was observed before SPB separation. This off-site location of the kinetochores implies that sister kinetochores at this stage are unable to serve as a fulcrum to generate a repulsive force through microtubules. After a while, the cnt1-GFP foci overlap with Sfi1-CFP when two SPBs separate (yellow bracket, Figure 4A; 60 s, Figure 4B). This correlation suggests that the location of the sister kinetochores is key for the generation of a repulsive force to trigger SPB separation.

Then, the relaxation of kinetochores in a bivalent during meiosis I was confirmed using the cnt1-GFP system (Figure 4, D and E). On entry into meiosis I, a radial array of microtubules was assembled to capture and reposition centromeres (Kakui *et al.*, 2013) in WT and *cut7Δ pkl1Δ* cells (Figure 4, D and E). Homologous kinetochores were often observed as two separate dots (for instance, Figure 4D; ~120 s; Supplemental Figure S4), reflecting that the linkage of homologues is based on chiasmata formed in the arm region of chromosomes, but not on the centromeric cohesion between homologues (Moore, 1998; Siomos and Nasmyth, 2003). In WT cells, SPB separation efficiently occurred using the standard Cut7-dependent machinery (Figure 4E). As the major machinery is absent in *cut7Δ pkl1Δ* cells, the homologous kinetochores eventually behaved separately and failed to be positioned together at SPBs (Figure 4D and Supplemental Figure S4). This visually demonstrates that homologous kinetochores are unable to serve as a fulcrum to generate a repulsive force to separate SPBs. Therefore, it was concluded that kinetochores generate an outward force in mitosis, but not efficiently in meiosis.

Centromeric cohesion is required for bipolar spindle assembly in *cut7Δ pkl1Δ* cells

In mitosis, sister kinetochores are tightly tethered by mitotic cohesin at centromeres (Tomonaga *et al.*, 2000; Bernard *et al.*, 2001; Nonaka *et al.*, 2002; Sakuno *et al.*, 2009) (WT, Figure 5A). It was assumed that in mitosis, the centromeric cohesion between sister chromatids

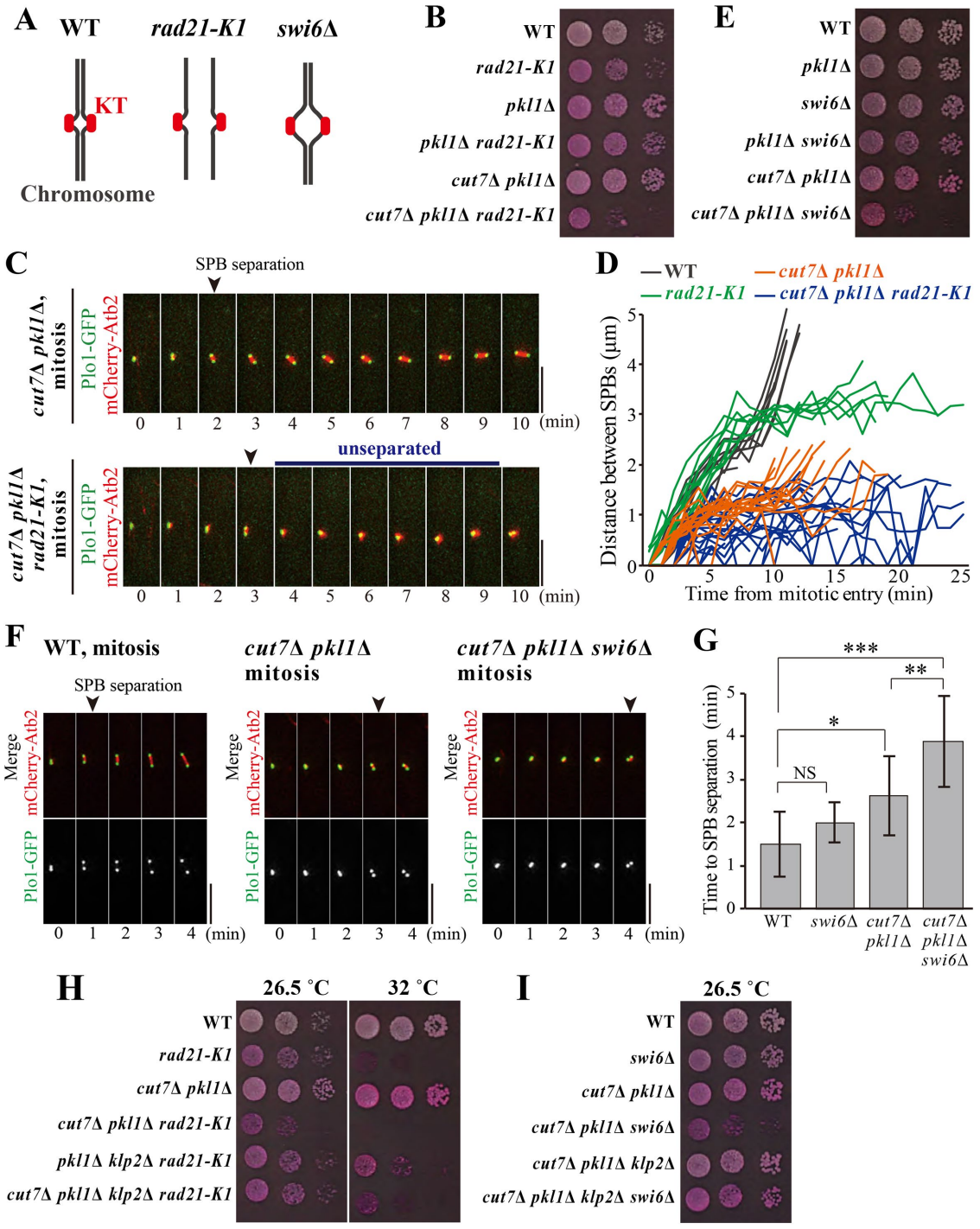

FIGURE 5: Centromeric cohesion is required for SPB separation in *cut7Δ pkl1Δ* cells. (A) Schematics for chromosome configurations in WT, *rad21-K1*, and *swi6Δ* cells in mitosis. (B) Strains with indicated genotypes were spotted onto agar plates to test their growth. Tenfold serial dilutions were spotted. The plates contained Phloxine B, which stains dead or sick cells. (C) Time-lapse images for mitotic cells of *cut7Δ pkl1Δ* and *cut7Δ pkl1Δ rad21-K1*. Microtubules and SPBs were visualized with mCherry-Atb2 and Plo1-GFP, respectively. Time 0 (min) corresponds to when a nuclear punctate signal of mCherry-Atb2 first emerged. The timing of SPB separation is indicated with arrowheads. (D) Temporal kinetics of the distance between two SPBs. Mitotic cells of WT (gray; $n = 10$ cells), *rad21-K1* (green; $n = 11$), *cut7Δ pkl1Δ* (orange; $n = 16$), and *cut7Δ pkl1Δ rad21-K1* (blue; $n = 24$) were observed at 36°C. (E) Plate-based growth assay as shown in B. (F) Time-lapse images of WT (left), *cut7Δ pkl1Δ* (center), or *cut7Δ pkl1Δ swi6Δ* cells (right) expressing Plo1-GFP (SPB; green) and mCherry-Atb2 (microtubules; red), as in C. The timing of SPB separation is indicated with arrowheads. (G) Time required for SPB separation since a nuclear punctate signal of mCherry-Atb2 first appeared (mean ± SD WT, $n = 8$ cells; *swi6Δ*, $n = 10$; *cut7Δ pkl1Δ*, $n = 18$; *cut7Δ pkl1Δ swi6Δ*, $n = 9$). $^*P < 0.01$; $^{**}P < 0.005$; $^{***}P < 0.001$; NS, not significant (Welch's *t* test). (H, I) Plate-based growth test using 10-fold serial dilutions of indicated strains as in B and E. Scale bars, 5 μm.

contributes to the generation of the outward repulsive force to separate SPBs in *cut7Δ pkl1Δ* cells.

The function of the mitotic cohesin Rad21 connecting the sister chromatids was impaired by introducing the *rad21-K1* temperature-sensitive hypomorphic mutation to test this assumption (Tatebayashi *et al.*, 1998) (Figure 5A). Indeed, at the restrictive temperature, the *rad21-K1* mutant precociously separated centromeres before the anaphase (Bernard *et al.*, 2001) (Supplemental Figure S5). The *rad21-K1* mutation was introduced to the *cut7Δ pkl1Δ* cells, and the triple mutant *cut7Δ pkl1Δ rad21-K1* showed a severe synthetic growth defect even at 26.5°C, whereas both *cut7Δ pkl1Δ* and *rad21-K1* mutants grew (Figure 5B).

The *cut7Δ pkl1Δ rad21-K1* mitotic cells visualizing microtubules and mitotic SPBs with mCherry-Atb2 and Plo1-GFP (Polo-like kinase) (Bähler *et al.*, 1998b), respectively, were then observed. In the majority of mitotic *cut7Δ pkl1Δ* cells, SPB separation occurred, and the distance between the two SPBs remained constant at ~1.5 μm for 5–10 min (Figure 5, C and D). On the contrary, the distance between SPBs fluctuated in the *cut7Δ pkl1Δ rad21-K1* cells. Two SPBs were located alongside each other most of the time during observation, and SPBs were reconnected even if once separated (Figure 5, C and D). These results imply that the impaired cohesion between sister chromatids is a reason for a loss of the outward force in the spindle.

In the *rad21-K1* mutant, cohesion between the sister chromatids was lost. To further specify whether cohesion at centromeres generates the outward tension, the *swi6Δ* strain was introduced to dismiss cohesin from the pericentromeric regions. Swi6/HP1 is a heterochromatin protein, which recruits cohesin to the pericentromeric regions (Ekwall *et al.*, 1995; Bernard *et al.*, 2001; Nonaka *et al.*, 2002). As reported previously, the core centromeres of sister chromatids (indicated by cnt1-GFP) behave in a discrete manner even before the anaphase in *swi6Δ* cells, confirming that the linkage between core centromeres is relaxed by the removal of Swi6 (Ekwall *et al.*, 1995; Bernard *et al.*, 2001; Nonaka *et al.*, 2002) (Figure 5A and Supplemental Figure S5D). When Swi6 was removed from the *cut7Δ pkl1Δ* strain, the *cut7Δ pkl1Δ swi6Δ* triple mutant showed severe growth defects, although neither *cut7Δ pkl1Δ* nor *swi6Δ* showed growth defects in these conditions (Figure 5E). The frequency of mitotic cells showing the short spindle (≤1.5 μm) increased when *swi6* was removed from *cut7Δ pkl1Δ* cells, which was comparable to when the *rad21-K1* mutation was introduced (Supplemental Figure S6).

In the live-cell imaging of WT cells, two SPBs separated and the bipolar spindle was stably assembled to a size of ~2 μm immediately after mitotic entry (1 min, WT; Figure 5F). SPB separation took longer in the *cut7Δ pkl1Δ* cells (3 min, Figure 5F), reflecting the reduction of outward forces for SPB separation. Furthermore, SPBs in *cut7Δ pkl1Δ swi6Δ* cells remained unseparated for longer than in the *cut7Δ pkl1Δ* cells (3.9 ± 1.1 min vs. 2.6 ± 0.9 min; Figure 5G), indicating that centromeric cohesion promotes SPB separation in the *cut7Δ pkl1Δ* mutant. This may mimic the chromosome state in meiosis I of the *cut7Δ pkl1Δ* cells, in which the outward force is not fully generated due to the relaxed connection between the homologous kinetochores. The defects in SPB separation in *cut7Δ pkl1Δ swi6Δ* cells were partial, probably because sister-centromeres were only partially loosened by the removal of Swi6.

As the force balance in meiosis I was ameliorated by the removal of the *klp2* gene from the *cut7Δ pkl1Δ* cells (Figure 2), it was reasoned by analogy that the deletion of *klp2* could suppress defects in *cut7Δ pkl1Δ swi6Δ* cells. As expected, the mitotic growth of both *cut7Δ pkl1Δ rad21-K1* and *cut7Δ pkl1Δ swi6Δ* cells was partially restored by the removal of the *klp2* gene (Figure 5, H and I). This implies that inward and outward forces inside the spindle are rebalanced there so that cells can assemble the bipolar spindle. These results demonstrate that centromeric cohesion contributes to generating the outward forces and bipolar spindle assembly in the absence of Cut7 and Pkl1.

The functional outer kinetochore is required for efficient SPB separation

Although the results using mutants of cohesin and Swi6 imply that centromeric cohesion could be key for generation of the outward force, it is alternatively possible that the merotelic attachment of microtubules to kinetochores impedes SPB separation, as such attachment is frequently observed in cohesin mutants (Courthéoux *et al.*, 2009). It was thought that the effects of merotelic attachment to SPB separation in pro-prometaphase are minor because merotelic attachment is thought to affect microtubule force balance, particularly in the anaphase when chromosomes with normal attachment have already finished segregation (Cimini *et al.*, 2004; Courthéoux *et al.*, 2009). Indeed, although *moa1Δ rec12Δ* often causes merotelic attachment, it restored SPB separation in *cut7Δ pkl1Δ* in pro-prometaphase, and spindle elongation defects could be seen only in the anaphase (see Figure 3B).

To further clarify this point, it is necessary to investigate more directly whether kinetochore generates the outward force for SPB separation through microtubules. Therefore, the mutant of Nuf2, a component of the Ndc80 complex located in the outer kinetochore, which serves as the interface for kinetochore-microtubule attachment, was employed (Wigge and Kilmartin, 2001). Then, the temperature-sensitive *nuf2-2* mutant (Nabetani *et al.*, 2001) was crossed with the *cut7Δ pkl1Δ* mutant to investigate whether SPB separation is affected by defective outer kinetochores.

The *cut7Δ pkl1Δ nuf2-2* cells were delayed in SPB separation at the onset of mitosis (Figure 6A). The *cut7Δ pkl1Δ* (*nuf2*$^{+}$) cells started to separate SPBs within 5 min after the mitotic onset, whereas more than 25% of the *cut7Δ pkl1Δ nuf2-2* cells did not separate SPBs within 5 min (Figure 6, B and C). Once SPBs were separated, the spindle was occasionally longer than 1 μm. As the *nuf2-2* mutant is not completely null, the effects of the mutation might be partial. Nonetheless, the *nuf2-2* mutation caused severe delays in the initial stage of SPB separation in *cut7Δ pkl1Δ* cells, indicating that the outer kinetochore complex plays a central role in SPB separation.

This was also tested in meiosis I. As shown above, *cut7Δ pkl1Δ klp2Δ* cells showed SPB separation in meiosis I (Figures 2, B and C, and 6D), but *cut7Δ pkl1Δ klp2Δ nuf2-2* cells were mostly defective in SPB separation at meiosis I (Figure 6, D and E). Therefore, it is concluded that SPB separation in meiosis I in the absence of kinesin-5 (Cut7) and both kinesin-14s (Pkl1 and Klp2) depends on kinetochore-microtubule attachment through the outer kinetochore complex.

DISCUSSION

The outward force mediated by kinetochores

Visualization of kinetochores and the genetic experiments demonstrate that the tight connection between sister kinetochores as well as the functional outer kinetochore complex are the bases for a repulsive outward force for microtubules to separate SPBs. This is particularly evident in *cut7Δ pkl1Δ* cells lacking two opposing kinesins (Figure 7). It is proposed that kinetochores contribute to the generation of outward forces for SPB separation in mitosis, but kinetochores fail to do so in meiosis I, because the interkinetochore tension in a meiotic bivalent (i.e., between homologous

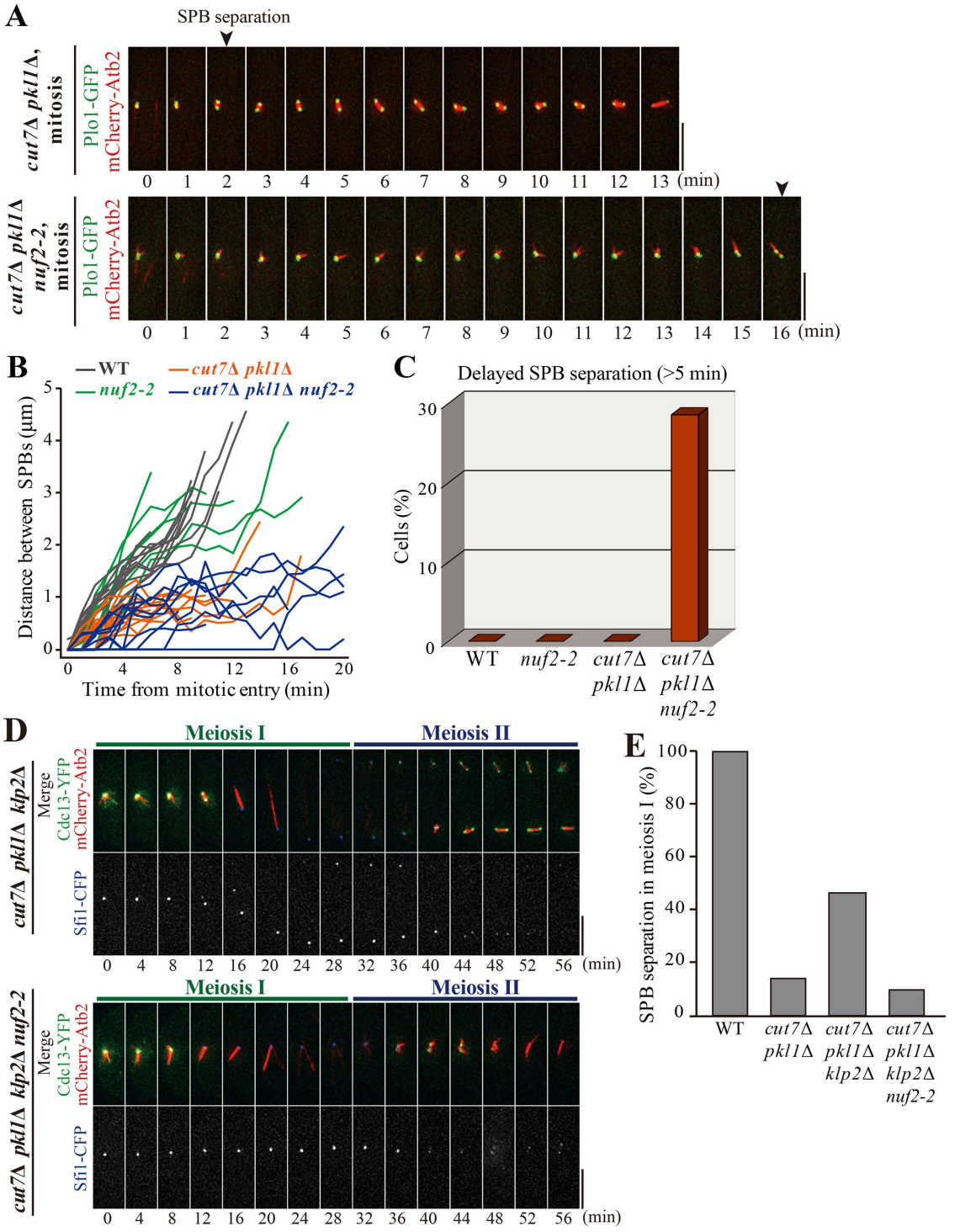

FIGURE 6: Functional kinetochore is required for generation of the outward force. (A) Time-lapse images of Plo1-GFP and mCherry-Atb2 in the mitosis of *cut7Δ pkl1Δ* cells and *cut7Δ pkl1Δ nuf2-2* cells at 36°C. Arrowheads indicate the timing of SPB separation. Time 0 corresponds to the onset of mitosis. (B) Kinetics of distance between two SPBs in indicated strains. (C) Percentages of cells with delayed SPB separation in each strain. Mitotic cells in which SPBs did not separate for more than 5 min after the mitotic onset are counted (WT, $n = 16$ cells; *nuf2-2*, $n = 7$; *cut7Δ pkl1Δ*, $n = 20$; *cut7Δ pkl1Δ nuf2-2*, $n = 14$). (D) Cells expressing Cdc13-YFP (green), mCherry-Atb2 (microtubules; red), and Sfi1-CFP (SPB; blue) were observed at 36°C from the onset of meiosis I in *cut7Δ pkl1Δ klp2Δ* (top) and *cut7Δ pkl1Δ klp2Δ nuf2-2* (bottom). (E) Percentages of cells that showed SPB separation in meiosis I in indicated strains, as calculated from observations in D (WT, $n = 8$ cells; *cut7Δ pkl1Δ*, $n = 14$; *cut7Δ pkl1Δ klp2Δ*, $n = 15$; *cut7Δ pkl1Δ klp2Δ nuf2-2*, $n = 10$). Scale bars, 5 μm.

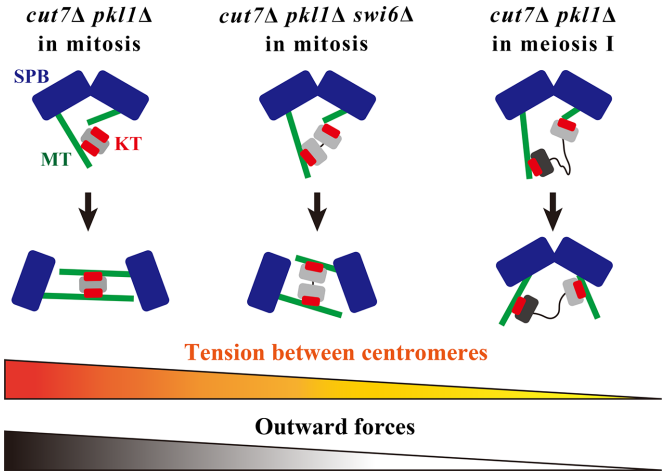

FIGURE 7: Model for the relationship between centromeric cohesion and the outward force to separate SPBs in *cut7Δ pkl1Δ*. The behavior of kinetochores and SPBs in *cut7Δ pkl1Δ* mitotic cells (left), *cut7Δ pkl1Δ swi6Δ* mitotic cells (center), and *cut7Δ pkl1Δ* cells in meiosis I (right) are shown. Gray and black ovals denote a pair of homologous chromosomes. Wavy lines indicate that the connection between the chromosomes is relaxed. See text for details.

kinetochores but not sister kinetochores) is low, compared with that in a mitotic univalent (Figure 7). SPBs in *cut7Δ pkl1Δ* cells were separated later in meiosis II, in which kinetochore configuration is reconverted to mitotic style (bioriented kinetochores in a univalent). Moreover, the artificial conversion of kinetochore geometry in meiosis I from the mono-oriented to mitotic bioriented style (by use of *moa1Δ* and *rec12Δ moa1Δ*) partially restored SPB separation (Figure 3, A–D, and Supplemental Figure S3, A–C). Therefore, it is concluded that the kinetochore-mediated outward force is relatively low in meiosis I due to the loose linkages between homologues (Figure 7).

Balance of inward and outward forces

As previously shown in studies on *S. pombe* mitosis, SPB separation is orchestrated by a number of outward and inward forces within the spindle (Pidoux *et al.*,1996; Rincon *et al.*, 2017; Yukawa *et al.*, 2017). In the presence of Cut7, the *rad21-K1*, *swi6Δ*, and *nuf2-2* single mutants separated SPBs almost normally (Figures 5, D and G, and 6B). Therefore, Cut7 appears to be the major outward-force generator that cross-links and slides microtubules in WT cells, and the kinetochore may serve as an additional factor to further assist the outward force.

In the absence of both Cut7 and Pkl1 in mitosis, outward forces dominate and therefore SPBs are separated. Tight cohesion of sister kinetochores contributes to the generation of the outward forces for efficient SPB separation.

However, in meiosis I, the outward forces do not dominate. SPBs do not separate in the double knockout, because kinetochores in a bivalent are loosely connected. Recent studies indicate that the microtubule-bundling factor Ase1 is responsible for the generation of the outward force that separates SPBs in the absence of both Cut7 and Pkl1 (Rincon *et al.*, 2017; Yukawa *et al.*, 2017). Based on this notion, defects in SPB separation in meiosis I could be interpreted as an absence of Ase1 functions at this stage. Inward forces driven by Klp2 (Yukawa *et al.*, 2018) might be stronger than in mitosis to hold back SPB separation, or Ase1 might not fully function in meiosis I, although those possibilities are not mutually exclusive.

Indeed, the removal of Klp2 in *cut7Δ pkl1Δ* cells restored SPB separation, supporting this notion. Regarding Ase1, it is speculated that the transient bilateral attachment of kinetochores to microtubules generates the interlock of antiparallel microtubules (see Figure 7), thereby providing a base for Ase1 localization to promote SPB separation. In meiosis I of the *cut7Δ pkl1Δ* cells, flexible cohesion in a bivalent does not produce sufficient interdigitating microtubules. Therefore, Ase1 might not be able to fully function at this stage.

Lack of the kinetochore-mediated outward force in meiosis I

Kinetochore positioning in the nucleus is regulated distinctly in mitosis and meiosis. In the interphase of the mitotic cell cycle, kinetochores are tethered at SPBs in the nucleus (Funabiki *et al.*, 1993). Therefore, it is reasonable to utilize kinetochores as a pivot point for bipolar spindle assembly when spindle microtubules are emanated from SPBs on entry into mitosis.

In contrast, kinetochores locate distal from SPBs and are scattered in the nucleus before entry into meiosis I (Chikashige *et al.*, 1994). They are repositioned at the onset of meiosis I since distal kinetochores are captured and retrieved by a radial array of microtubules assembled from unseparated SPBs (Kakui *et al.*, 2013).

As the radial array is reminiscent of the monopolar "V-shaped" spindle seen in mitosis of the *cut7* hypomorphic mutant (Hagan and Yanagida, 1990), the radial array of microtubules in meiosis may need to be assembled from unseparated SPBs that are juxtaposed to each other.

In this study, two possible explanations have been identified as to how the monopolar radial array of microtubules are assembled specifically at the onset of meiosis I. First, it is possible that Cut7 is not fully functional at the onset of meiosis I, although Cut7 is localized to SPBs at this stage (unpublished data). The other possibility, although not mutually exclusive, is that the meiosis-specific configuration of chromosomes prevents SPB separation, thereby assisting the assembly of the monopolar radial array of microtubules. Kinetochores in meiosis I are connected loosely in a bivalent and are distal from SPBs. These circumstances do not allow the generation of kinetochore-mediated outward forces that promote SPB separation. This brings a substantial delay in SPB separation, which promotes the assembly of the monopolar array of microtubules instead, thereby providing an opportunity for kinetochore repositioning. SPBs then start to separate as soon as the radial array diminishes (Kakui *et al.*, 2013).

Moreover, the close proximity of kinetochores and SPBs promotes bipolar spindle assembly in meiosis I (Fennell *et al.*, 2015). These observations indicate that although meiotic kinetochores in a bivalent are relaxed, kinetochores contribute to separate SPBs, albeit partially, as soon as they are retrieved to SPBs. Therefore, the positioning and configuration of kinetochores control the timing of SPB separation.

MATERIALS AND METHODS

Yeast strains, media, and genetics

S. pombe strains used in this study are listed in Supplemental Table S1. For vegetative growth, cells were grown in the rich medium YE5S containing yeast extract, glucose, and five supplements (adenine, leucine, uracil, lysine, and histidine). To induce mating, meiosis, and sporulation, homothallic (h^{90}) cells were grown in YE5S and then spotted onto sporulation agar (SPA) plates. For plate-based growth assays, 10-fold serial dilutions of cell suspensions (ranging from 1×10^4 to 1×10^2 cells) were spotted onto YE5S plates with or without Phloxine B. The plates were incubated at 26.5°C or 32°C. Standard methods for yeast genetics and PCR-based gene targeting for gene deletion and the tagging of fluorescent proteins

were used (Moreno *et al.*, 1991; Bähler *et al.*, 1998a; Sato *et al.*, 2005, 2009). For the visualization of microtubules, the fusion gene of *mCherry* and *atb2* (α2-tubulin) placed under the native promoter and terminator of the *atb2*$^+$ gene was integrated into a chromosome as an extra copy of endogenous *atb2*$^+$(the resultant strain is referred to as "*Z2-mCherry-atb2*") (Ohta *et al.*, 2012).

Microscopy

Cells on SPA (for 24 h) were fixed with ethanol and then mounted on the glass slide using VECTASHIELD mounting medium with DAPI (Vector Laboratories) to visualize DNA in spores. Cells were spotted onto SPA and incubated at 30°C for 18 h and fixed with 3.2% formaldehyde (FUJIFILM Wako Pure Chemical) and mounted similarly to visualize DNA in the *mes1*Δ mutant. Images were taken using the DeltaVision-SoftWoRx system (Applied Precision).

For the live-cell imaging of meiotic cells, homothallic cells were spotted onto SPA and incubated at 30°C for 7–10 h, except for the *nuf2-2* strains incubated on SPA at 30°C for 5 h and shifted to 36°C for 2 h prior to observation. For the observation of mitosis, most of the strains were cultured in the YE5S liquid medium until the mid–log phase at 30°C. Exceptionally, the *rad21-K1* and *nuf2-2* strains were cultured in the YE5S liquid medium at 25°C and shifted to 36°C for 2.5 h (*rad21-K1*) or 4 h (*nuf2-2*) prior to observation. Cells were then mounted on a glass-bottom dish (Iwaki glass) precoated with lectin from Glycine max (Sigma) and filled with a synthetic medium with adenine, leucine, uracil, lysine, and histidine (SD5S) for the observation of mitosis, alternatively with minimal medium without a nitrogen source supplemented with uracil and leucine for meiosis. Filming was performed using the DeltaVision-SoftWoRx system (Applied Precision) as described previously (Sato *et al.*, 2009). The *rad21-K1* and *nuf2-2* mutants were incubated at 36°C during observation. Images were acquired as serial sections along the *z*-axis and stacked using the quick projection algorithm in SoftWoRx. Kymographs were generated using the SoftWoRx software, and image contrasts were adjusted with Adobe Photoshop CC 2019.

Immunofluorescence

Cells were cultured in the YE5S liquid medium until the mid–log phase at 25°C and then shifted up to 36°C. After 4 h, cells were fixed with 3.2% formaldehyde (FUJIFILM Wako Pure Chemical). Samples were then stained with the mouse anti–α-tubulin antibody B-5-1-2 (Santa Cruz Biotechnology) as a primary antibody and with Goat anti-mouse immunoglobulin G (H+L) Cross-Adsorbed Secondary Antibody, Alexa Fluor 594 (Thermo Fisher Scientific). The samples were then sealed with VECTASHIELD mounting medium with DAPI (Vector Laboratories).

Statistical analysis

Welch's *t* test was used to evaluate the statistical significance of the difference between two values. All data are presented as the mean ± SD.

ACKNOWLEDGMENTS

We thank Yasushi Hiraoka, Takeshi Sakuno, Yoshinori Watanabe, Yasutaka Kakui, and the National Bioresource Project of Japan for strains. We are grateful to Mika Toya for discussion. This work was supported by Japan Society for the Promotion of Science (JSPS) KAKENHI JP25291041, JP15H01359, JP16H04787, JP16H01317, and JP18K19347 to M.S. This study was also supported by The Uehara Memorial Foundation and by Waseda University grants for Special Research Projects 2017B-242, 2017B-243, 2018B-222, and 2019C-570 to M.S. This work was partly supported by the JSPS Core-to-Core Program, A.Advanced Research Networks.

REFERENCES

Bähler J, Wu JQ, Longtine MS, Shah NG, McKenzie A 3rd, Steever AB, Wach A, Philippsen P, Pringle JR (1998a). Heterologous modules for efficient and versatile PCR-based gene targeting in *Schizosaccharomyces pombe*. Yeast 14, 943–951.

Bähler J, Steever AB, Wang YL, Pringle JR, Gould KL (1998b). Role of polo kinase and Mid1p in determining the site of cell division in fission yeast. J Cell Biol 143, 1603–1616.

Bernard P, Maure JF, Javerzat JP (2001). Fission yeast Bub1 is essential in setting up the meiotic pattern of chromosome segregation. Nat Cell Biol 3, 522–526.

Bresch C, Muller G, Egel R (1968). Genes involved in meiosis and sporulation of a yeast. Mol Gen Genet 102, 301–306.

Cao L, Alani E, Kleckner N (1990). A pathway for generation and processing of double-strand breaks during meiotic recombination in S. cerevisiae. Cell 61, 1089–1101.

Cervantes MD, Farah JA, Smith GR (2000). Meiotic DNA breaks associated with recombination in *S. pombe*. Mol Cell 5, 883–888.

Chikashige Y, Ding DQ, Funabiki H, Haraguchi T, Mashiko S, Yanagida M, Hiraoka Y (1994). Telomere-led premeiotic chromosome movement in fission yeast. Science 264, 270–273.

Cimini D, Cameron LA, Salmon ED (2004). Anaphase spindle mechanics prevent mis-segregation of merotelically oriented chromosomes. Curr Biol 14, 2149–2155.

Courthéoux T, Gay G, Gachet Y, Tournier S (2009). Ase1/Prc1-dependent spindle elongation corrects merotely during anaphase in fission yeast. J Cell Biol 187, 399–412.

Decottignies A, Zarzov P, Nurse P (2001). In vivo localisation of fission yeast cyclin-dependent kinase cdc2p and cyclin B cdc13p during mitosis and meiosis. J Cell Sci 114, 2627–2640.

Ekwall K, Javerzat JP, Lorentz A, Schmidt H, Cranston G, Allshire R (1995). The chromodomain protein Swi6: a key component at fission yeast centromeres. Science 269, 1429–1431.

Fennell A, Fernández-Álvarez A, Tomita K, Cooper JP (2015). Telomeres and centromeres have interchangeable roles in promoting meiotic spindle formation. J Cell Biol 208, 415–428.

Ferenz NP, Paul R, Fagerstrom C, Mogilner A, Wadsworth P (2009). Dynein antagonizes eg5 by crosslinking and sliding antiparallel microtubules. Curr Biol 19, 1833–1838.

Funabiki H, Hagan I, Uzawa S, Yanagida M (1993). Cell cycle-dependent specific positioning and clustering of centromeres and telomeres in fission yeast. J Cell Biol 121, 961–976.

Hagan I, Yanagida M (1990). Novel potential mitotic motor protein encoded by the fission yeast *cut7*$^+$ gene. Nature 347, 563–566.

Hagan I, Yanagida M (1992). Kinesin-related cut7 protein associates with mitotic and meiotic spindles in fission yeast. Nature 356, 74–76.

Heck MM, Pereira A, Pesavento P, Yannoni Y, Spradling AC, Goldstein LS (1993). The kinesin-like protein KLP61F is essential for mitosis in *Drosophila*. J Cell Biol 123, 665–679.

Izawa D, Goto M, Yamashita A, Yamano H, Yamamoto M (2005). Fission yeast Mes1p ensures the onset of meiosis II by blocking degradation of cyclin Cdc13p. Nature 434, 529–533.

Kakui Y, Sato M, Okada N, Toda T, Yamamoto M (2013). Microtubules and Alp7-Alp14 (TACC-TOG) reposition chromosomes before meiotic segregation. Nat Cell Biol 15, 786–796.

Kapitein LC, Peterman EJG, Kwok BH, Kim JH, Kapoor TM, Schmidt CF (2005). The bipolar mitotic kinesin Eg5 moves on both microtubules that it crosslinks. Nature 435, 114–118.

Kapoor TM, Mayer TU, Coughlin ML, Mitchison TJ (2000). Probing spindle assembly mechanisms with monastrol, a small molecule inhibitor of the mitotic kinesin, Eg5. J Cell Biol 150, 975–988.

Kashina AS, Baskin RJ, Cole DG, Wedaman KP, Saxton WM, Scholey JM (1996). A bipolar kinesin. Nature 379, 270–272.

Keeney S, Giroux CN, Kleckner N (1997). Meiosis-specific DNA double-strand breaks are catalyzed by Spo11, a member of a widely conserved protein family. Cell 88, 375–384.

Kilmartin JV (2003). Sfi1p has conserved centrin-binding sites and an essential function in budding yeast spindle pole body duplication. J Cell Biol 162, 1211–1221.

Lin Y, Smith GR (1994). Transient, meiosis-induced expression of the *rec6* and *rec12* genes of *Schizosaccharomyces pombe*. Genetics 136, 769–779.

Loïodice I, Staub J, Setty TG, Nguyen N-PT, Paoletti A, Tran PT (2005). Ase1p organizes antiparallel microtubule arrays during interphase and mitosis in fission yeast. Mol Biol Cell 16, 1756–1768.
Mayer TU, Kapoor TM, Haggarty SJ, King RW, Schreiber SL, Mitchison TJ (1999). Small molecule inhibitor of mitotic spindle bipolarity identified in a phenotype-based screen. Science 286, 971–974.
Mitchison TJ, Maddox P, Gaetz J, Groen A, Shirasu M, Desai A, Salmon ED, Kapoor TM (2005). Roles of polymerization dynamics, opposed motors, and a tensile element in governing the length of *Xenopus* extract meiotic spindles. Mol Biol Cell 16, 3064–3076.
Moore DP (1998). Chromosome segregation during meiosis: building an unambivalent bivalent. Curr Top Dev Biol 37, 263–299.
Moreno S, Klar A, Nurse P (1991). Molecular genetic analysis of fission yeast *Schizosaccharomyces pombe*. Methods Enzymol 194, 795–823.
Nabetani A, Koujin T, Tsutsumi C, Haraguchi T, Hiraoka Y (2001). A conserved protein, Nuf2, is implicated in connecting the centromere to the spindle during chromosome segregation: a link between the kinetochore function and the spindle checkpoint. Chromosoma 110, 322–334.
Nicklas RB (1974). Chromosome segregation mechanisms. Genetics 78, 205–213.
Nonaka N, Kitajima T, Yokobayashi S, Xiao G, Yamamoto M, Grewal SIS, Watanabe Y (2002). Recruitment of cohesin to heterochromatic regions by Swi6/HP1 in fission yeast. Nat Cell Biol 4, 89–93.
Ohta M, Sato M, Yamamoto M (2012). Spindle pole body components are reorganized during fission yeast meiosis. Mol Biol Cell 23, 1799–1811.
Olmsted ZT, Colliver AG, Riehlman TD, Paluh JL (2014). Kinesin-14 and kinesin-5 antagonistically regulate microtubule nucleation by γ-TuRC in yeast and human cells. Nat Commun 5, 5339.
Pidoux AL, LeDizet M, Cande WZ (1996). Fission yeast pkl1 is a kinesin-related protein involved in mitotic spindle function. Mol Biol Cell 7, 1639–1655.
Rincon SA, Lamson A, Blackwell R, Syrovatkina V, Fraisier V, Tran PT (2017). Kinesin-5-independent mitotic spindle assembly requires the antiparallel microtubule crosslinker Ase1 in fission yeast. Nat Commun 8, 15286.
Sakuno T, Tada K, Watanabe Y (2009). Kinetochore geometry defined by cohesion within the centromere. Nature 458, 852–858.
Sakuno T, Tanaka K, Hauf S, Watanabe Y (2011). Repositioning of aurora B promoted by chiasmata ensures sister chromatid mono-orientation in meiosis I. Dev Cell 21, 534–545.
Sato M, Dhut S, Toda T (2005). New drug-resistant cassettes for gene disruption and epitope tagging in *Schizosaccharomyces pombe*. Yeast 22, 583–591.
Sato M, Toya M, Toda T (2009). Visualization of fluorescence-tagged proteins in fission yeast: the analysis of mitotic spindle dynamics using GFP-tubulin under the native promoter. Methods Mol Biol 545, 185–203.
Sharp DJ, Yu KR, Sisson JC, Sullivan W, Scholey JM (1999). Antagonistic microtubule-sliding motors position mitotic centrosomes in *Drosophila* early embryos. Nat Cell Biol 1, 51–54.
Siomos MF, Nasmyth K (2003). Un ménage à quatre: the molecular biology of chromosome segregation in meiosis. Cell 112, 423–440.
Tanenbaum ME, Macůrek L, Galjart N, Medema RH (2008). Dynein, Lis1 and CLIP-170 counteract Eg5-dependent centrosome separation during bipolar spindle assembly. EMBO J 27, 3235–3245.
Tatebayashi K, Kato J, Ikeda H (1998). Isolation of a *Schizosaccharomyces pombe rad21*^{ts} mutant that is aberrant in chromosome segregation, microtubule function, DNA repair and sensitive to hydroxyurea: possible involvement of Rad21 in ubiquitin-mediated proteolysis. Genetics 148, 49–57.
Tomonaga T, Nagao K, Kawasaki Y, Furuya K, Murakami A, Morishita J, Yuasa T, Sutani T, Kearsey SE, Uhlmann F, *et al*. (2000). Characterization of fission yeast cohesin: essential anaphase proteolysis of Rad21 phosphorylated in the S phase. Genes Dev 14, 2757–2770.
Troxell CL, Sweezy MA, West RR, Reed KD, Carson BD, Pidoux AL, Cande WZ, McIntosh JR (2001). *pkl1*$^{+}$and *klp2*$^{+}$: Two kinesins of the Kar3 subfamily in fission yeast perform different functions in both mitosis and meiosis. Mol Biol Cell 12, 3476–3488.
van Heesbeen RGHP, Tanenbaum ME, Medema RH (2014). Balanced activity of three mitotic motors is required for bipolar spindle assembly and chromosome segregation. Cell Rep 8, 948–956.
Wigge PA, Kilmartin JV (2001). The Ndc80p complex from *Saccharomyces cerevisiae* contains conserved centromere components and has a function in chromosome segregation. J Cell Biol 152, 349–360.
Yamagishi Y, Sakuno T, Goto Y, Watanabe Y (2014). Kinetochore composition and its function: lessons from yeasts. FEMS Microbiol Rev 38, 185–200.
Yamashita A, Fujita A, Yamamoto M (2005). The roles of fission yeast Ase1 in mitotic cell division, meiotic nuclear oscillation, and cytokinesis checkpoint signaling. Mol Biol Cell 16, 1378–1395.
Yokobayashi S, Watanabe Y (2005). The kinetochore protein Moa1 enables cohesion-mediated monopolar attachment at meiosis I. Cell 123, 803–817.
Yukawa M, Kawakami T, Okazaki M, Kume K, Tang NH, Toda T (2017). A microtubule polymerase cooperates with the kinesin-6 motor and a microtubule cross-linker to promote bipolar spindle assembly in the absence of kinesin-5 and kinesin-14 in fission yeast. Mol Biol Cell 28, 3647–3659.
Yukawa M, Yamada Y, Toda T (2019). Suppressor analysis uncovers that MAPs and microtubule dynamics balance with the Cut7/Kinesin-5 motor for mitotic spindle assembly in *Schizosaccharomyces pombe*. G3 (Bethesda) 9, 269–280.
Yukawa M, Yamada Y, Yamauchi T, Toda T (2018). Two spatially distinct kinesin-14 proteins, Pkl1 and Klp2, generate collaborative inward forces against kinesin-5 Cut7 in *S. pombe*. J Cell Sci 131, jcs210740.